

# RSC Advances



This is an *Accepted Manuscript*, which has been through the Royal Society of Chemistry peer review process and has been accepted for publication.

*Accepted Manuscripts* are published online shortly after acceptance, before technical editing, formatting and proof reading. Using this free service, authors can make their results available to the community, in citable form, before we publish the edited article. This *Accepted Manuscript* will be replaced by the edited, formatted and paginated article as soon as this is available.

You can find more information about *Accepted Manuscripts* in the [Information for Authors](#).

Please note that technical editing may introduce minor changes to the text and/or graphics, which may alter content. The journal's standard [Terms & Conditions](#) and the [Ethical guidelines](#) still apply. In no event shall the Royal Society of Chemistry be held responsible for any errors or omissions in this *Accepted Manuscript* or any consequences arising from the use of any information it contains.



Journal Name

COMMUNICATION

## Spiral Growth Mode in DMDPC Organic Thin Film Transistors by Physical Vapor Deposition

Received 00th January 20xx,  
Accepted 00th January 20xx

Tianjun Liu,<sup>a,b</sup> Jiawei Wang,<sup>a,b</sup> Liang Wang,<sup>a</sup> Jing Wang,<sup>c</sup> Jingbo Lan,<sup>c</sup> Jingsong You<sup>c</sup> and Chao Jiang<sup>\*a</sup>

DOI: 10.1039/x0xx00000x

www.rsc.org/

**We report the observation of a screw-dislocation-driven spiral growth of DMDPC organic thin films using a physical vapor deposition. The existence of screw dislocations was clearly confirmed by the observations of outcropped steps, single monolayer height helical periodicity and spiral fringes.**

Organic thin film transistors (OTFTs) have attracted considerable interest due to their potential applications in flexible, low cost and large area devices such as displays,<sup>1</sup> sensors,<sup>2</sup> and organic complementary circuits.<sup>3</sup> In the last decade, tremendous progress has been made in the synthesis of n- and p-channel organic semiconductors and the charge carrier mobilities have reached a new level of above  $10 \text{ cm}^2 \text{ V}^{-1} \text{ s}^{-1}$ .<sup>4</sup> The performance of organic semiconductors is directly related to the molecular packing, crystallinity, growth mode and purity.<sup>5</sup> Nonetheless, in OTFTs, because the induced charges in the conducting channel reside with the first several monolayers near the interface between semiconductor and dielectric,<sup>6</sup> the growth and crystalline order of these interfacial layers are deadly crucial to the transistor performance.<sup>7</sup>

Generally, the growth mode is determined by a competition between interlayer interaction and molecule substrate interaction energies.<sup>8</sup> In the case of organic molecular films such as pentacene, C<sub>8</sub>-BTBT, etc.,<sup>9</sup> the interactions between molecules are weak van der Waals interactions, so that their first monolayer tends to form consecutive crystalline domains before a second layer starts to grow.<sup>10</sup> Also many other molecules were designed to achieve high mobility and good stability through chemical structural

modification.<sup>11, 12</sup> However, film growth of those molecules other than simple structured and/or functionalized with substitute groups does not always obey the layer-by-layer (or S-K mode for pentacene) two-dimensional (2D) growth mode. If under an un-optimized growth condition, three-dimensional (3D) nucleation and even amorphous modes occur, which are harmful to charge transport in thin film transistors.<sup>13</sup> On the other hands, when the system is under a low supersaturation, an initial growth tends to convert into a defect-assisted growth mode: the spiral terrace growth mode where adatoms easily swept fast across the terrace to arrive at the edge of the island.<sup>10</sup> Compared with 3D nucleation grains and amorphous growth, it is favourable to adopt the spiral growth mode if a molecule cannot be grown by a 2D layer-by-layer growth, since large lateral grain size under the spiral growth may be favorite to the grain connection and facilitates to the charge transport along the conduction channel.

In inorganic materials, the screw dislocation driven (SDD) growth was discussed in 2D layered materials and nanotubes before.<sup>14-17</sup> For a molecular thin film growth, the observations of spiral growth driven by dislocations were seldom reported. Here, we demonstrate that spirals in organic thin films involving screw terraces can be directly grown using physical vapor deposition (PVD). A thorough investigation for small molecule DMDPC is carried out systematically to control thin film growth and minimize detrimental grain boundaries, and substrate modification as well as optimization of growth parameters such as deposition rate, film thickness and substrate temperature are applied to fabricate a field effect transistor.

a. CAS Key Laboratory of Standardization and Measurement for Nanotechnology, and CAS Center for Excellence in Nanoscience, National Center for Nanoscience and Technology, No. 11 Beiyitiao Zhongguancun, Beijing 100190, China

b. University of Chinese Academy of Sciences, No. 19A Yuquan Road, Beijing 100049, China

c. Key Laboratory of Green Chemistry and Technology of Ministry of Education, College of Chemistry, and State Key Laboratory of Biotherapy, West China Medical School, Sichuan University, 29 Wangjiang Road, Chengdu 610064, P. R. China. Email: Jiangch@nanoctr.cn

Electronic Supplementary Information (ESI) available: [details of any supplementary information available should be included here]. See DOI: 10.1039/x0xx00000x

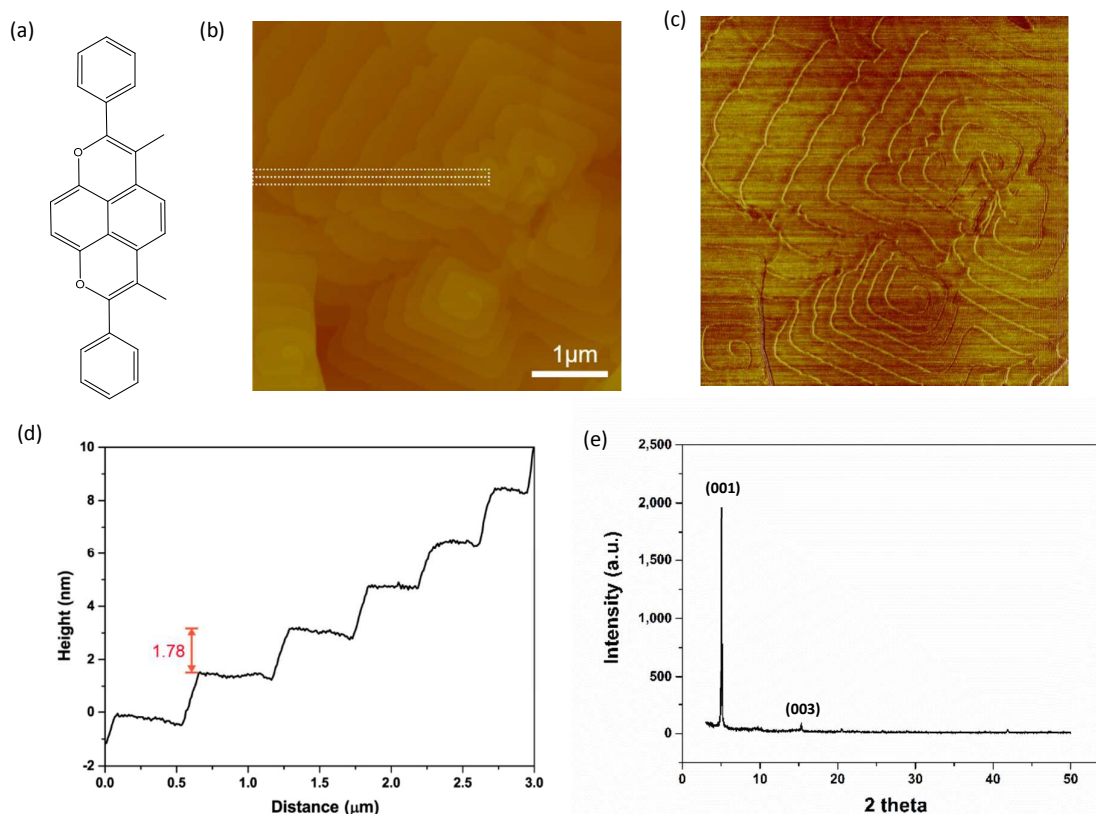


Fig.1 (a) the chemical structure of DMDPC, (b)  $5\mu\text{m} \times 5\mu\text{m}$  AFM height image of DMDPC films namely thickness 45nm on OTS treated  $\text{Si}/\text{SiO}_2$ , (c) AFM force image showing obvious helical fringes, (d) AFM height profile of DMDPC films along the white line in (b). (e) XRD pattern of the 45nm DMDPC films on OTS treated substrate.

In this work, we use the conjugated molecule 3,6-dimethyl-2,7-diphenylisochromeno[7,8,1-def]chromene (DMDPC) to grow the spirals, which was proved to be a type of red-emitting luminophore material for the application of sensors and OLEDs.<sup>18</sup> The chemical structure of DMDPC was shown in Figure 1a. N-type heavily doped silicon wafers with thermally grown 300nm thick  $\text{SiO}_2$  were used as substrates. The wafers were cleaned with piranha solution, followed by ultrasonic clean treatment in acetone, ethanol, deionized water. The surface of the wafers was modified with n-octyltrichlorosilane OTS SAM by vapor-deposition method. The DMDPC was evaporated onto  $\text{Si}/\text{SiO}_2$  substrate treated with OTS which decreases the number of surface trapping hydroxyl groups on bare  $\text{SiO}_2$  surface.<sup>19</sup> The DMDPC films were deposited in a thermal evaporation system Auto 306 (BOC-Edwards Co.). The deposition rate was controlled to be at 0.2nm/min. The substrate temperature was controlled by a ceramic heating plate integrated in AUTO 306. As the lower deposition rate and higher substrate temperature bring the system to low supersaturations where the priority growth mode is dislocation assisted growth.<sup>10</sup>

In general, each of these grains was constructed by stacking of spiral terraces on OTS treated substrate, while the

thin film morphology on bare  $\text{SiO}_2$  was tiny island sharp (see supporting information S1). To further explore the detailed structures of DMDPC thin films, we performed systematical atomic force microscope (AFM). Figure 1a shows the height image of the typical spiral growth observed in our samples, the step height of the terrace was 1.8nm, which matches the thickness of single molecular layer, as verified from the cross-section of height profiles labeled in Figure 1b (Figure 1d). The monolayer thickness could also be independently clarified by the X-ray diffraction (XRD). Figure 1e shows that the films exhibit two diffraction peaks at  $2\theta=5.04^\circ$  (d spacing=17.6Å) and  $2\theta=15.46^\circ$  (d spacing=5.74 Å), which are in agreement with the (001) and (003) diffractions derived from the single crystal structures. It shows that the film had a 17.6Å inter-planar distance perpendicular to the surface, which indicates that the 1.8nm step height is created by the DMDPC monolayer.

We further confirmed the DMDPC molecular initial growth process by depositing nominal 3nm thick films. Figure 2a-d show the AFM phase images of several separated spiral islands grown on OTS treated silicon substrate with size around 400nm (defined by the largest edge length of the grain). The 3D grain islands have different height range from

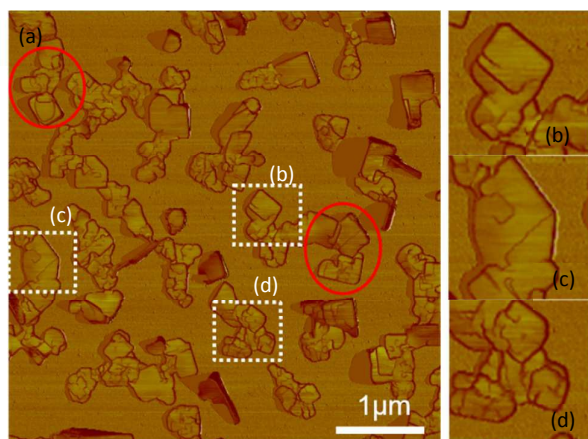


Fig.2 (a)  $5\mu\text{m} \times 5\mu\text{m}$  AFM force images analysis of DMDPC initial growth process. (b-d) different areas marked with white squares in (a).

3nm to 10nm. The outcrop steps can be clearly seen on each top of the grain, we were able to obtain that the original growth process is driven by the screw dislocation. Some grains close to each other would merge into a bigger one as shown in Figure 2a marked by red circle. This is reasonable for that the grains with the consistent molecules orientation would merge into a bigger one. Figure 3a gives a direct view of single grain with size  $600\text{nm} \times 600\text{nm}$ , the phase image can clearly show outcrop step and point of emergence. Further, we got higher-magnification AFM force image (Figure 3b) of the region marked by the black box in Figure 3a. We marked two different cross-section dash lines, I is far from the dislocation center and II is close to the dislocation center. The step height measured in line I and line II were 1.78nm and 1.18nm (Figure 3d, 3e), respectively. The monolayer step height is the elementary Burgers vector of the screw dislocation in the initial growth process were observed to further support that the DMDPC films followed a screw-dislocation-driven spiral growth mode.

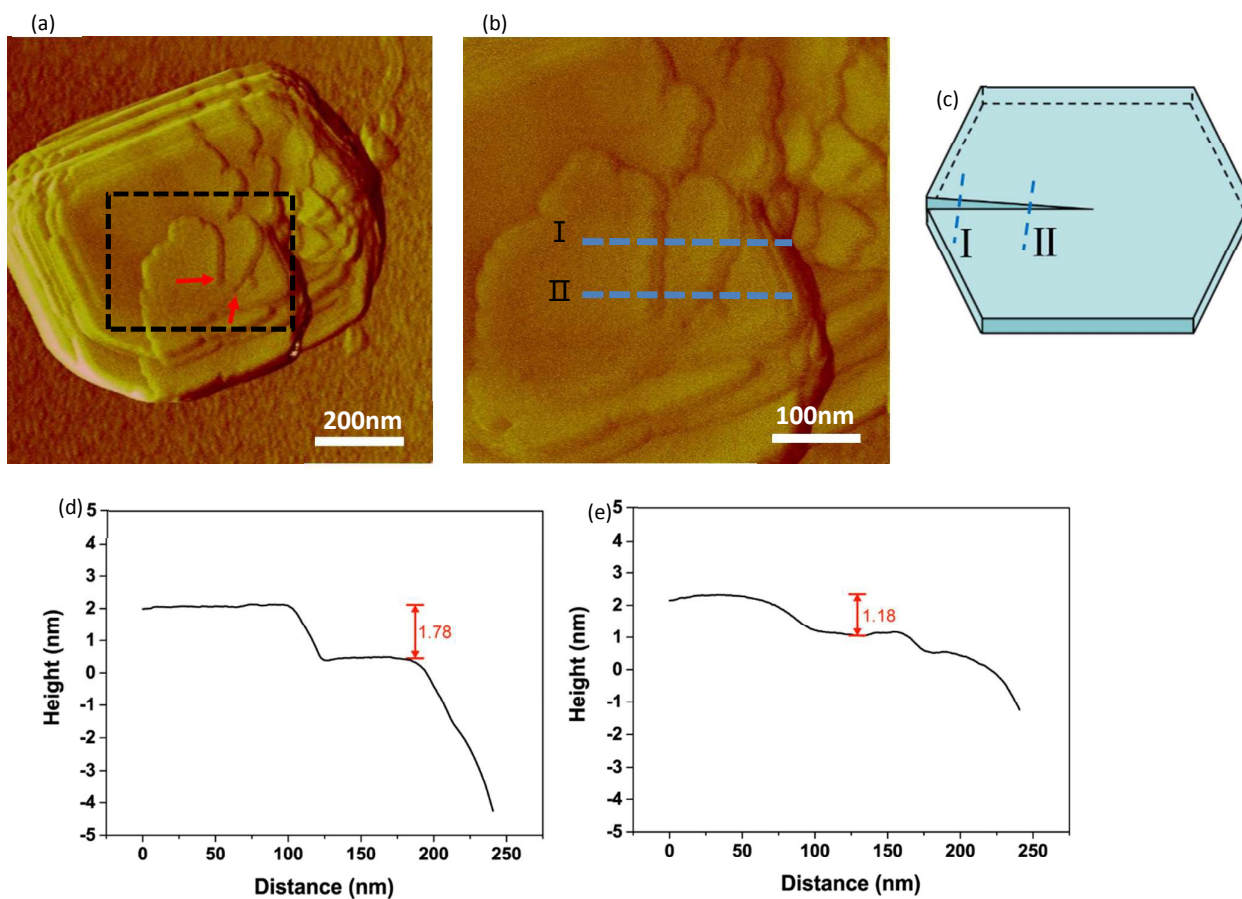


Figure 3. Characterization of outcrop monolayer step in DMDPC spirals. (a)  $1\mu\text{m} \times 1\mu\text{m}$  AFM force image of spiral grains, (b) Higher-magnification AFM phase image of the region marked by a black square in (a), (c) Schematic diagram show the outcrop step with monolayer height in a spiral grain, dash line I is far from the dislocation center and II is close to the dislocation center, (d) and (e) AFM height profile of outcrop steps marked by dash lines I and II, respectively.



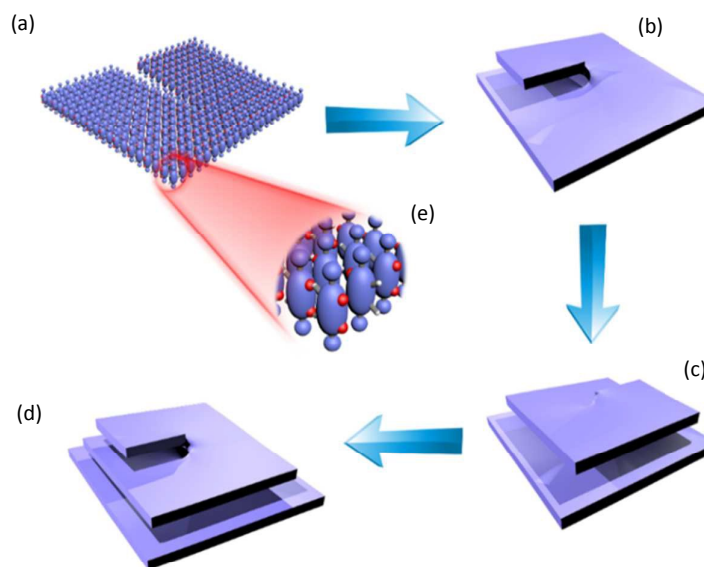


Figure 4. Growing mechanism of DMDPC films spirals. (a-d) schematic illustration of DMDPC spirals from nucleation to growth. The molecular packing model (e) the red circles represent oxygen and the grey stick is methyl.

Next, we investigate the growth mechanism for DMDPC spirals. In the low flux region, molecules diffuse along the surface and the growth mode is possible 2D layer-by-layer growth. However, nucleate new islands via 2D mode induce an energy barrier when a layer is completed.<sup>20</sup> Therefore, initial layer-by-layer growth tends to convert into a much faster and defect-assisted growth mode. According to BCF theory, the nucleation rate is very low and growth can occur at the existing surface steps associated with screw dislocations.<sup>21</sup> The formation of a screw dislocation core in DMDPC spirals requires the generation of slipped planes as the screw defects in the first monolayer, otherwise the growth will follow the 2D layer growth. We consider the case that a misfit dislocation at the grain boundary is possible origin of the spiral growth on OTS treated silicon substrate (shown in Figure 4a). According to the crystal structure, the DMDPC molecules adopt an “edge to face” stacking in a herringbone motif. Then each grid point has two DMDPC molecules with “face-to-face” packing structure, and the parallel molecules are centrosymmetric which the methyl side of one molecule is close to another’s oxygen side, as shown in Figure 4e, the red ball in one molecule is close to the grey ball in another molecule, where the red and the grey ball represent oxygen and methyl respectively. This kind of crystal structures in spiral growth were also reported recently.<sup>22</sup> Once the outcrop monolayer step is created, DMDPC molecules adsorbed on the terrace,

diffused and incorporated into kink sites, leading to the layer spreading laterally across the terrace.<sup>23</sup> As the layer spread laterally, next new layers are formed on top of terrace by the next turn of the spiral.<sup>24</sup> With a screw dislocation formed, it remains active and gradually grows in the vertical direction (shown in Figure 4b-d). Obviously, the emergence layers generated from a dislocation can grow on top of the bottom layers.<sup>23, 25</sup> On top of the spirals, the dislocation core can be clearly identified. We believe that this mechanism of spiral growth in organic films is not limited to DMDPC. Many other organic materials such as pentacene, C<sub>60</sub> and perylene share similar PVD growth mechanism.<sup>20, 26, 27</sup>

Since the DMDPC films were controllably spiral grown, it is significant to explore the charge transport behaviours. OFETs based on DMDPC were fabricated by employing the bottom-gate top-contact architecture. N-type heavily doped silicon wafers with thermally grown 300nm thick SiO<sub>2</sub> were used as substrates. The wafers were cleaned with piranha solution, followed by ultrasonic clean treatment in acetone, ethanol, deionized water. The surface of the wafers was modified with n-octyltrichlorosilane OTS SAM. The DMDPC films were deposited in a thermal evaporation system Auto 306 (BOC-Edwards Co.). The deposition rate was controlled to be at 0.2nm/min. The substrate temperature was controlled by a ceramic heating plate integrated in AUTO 306.

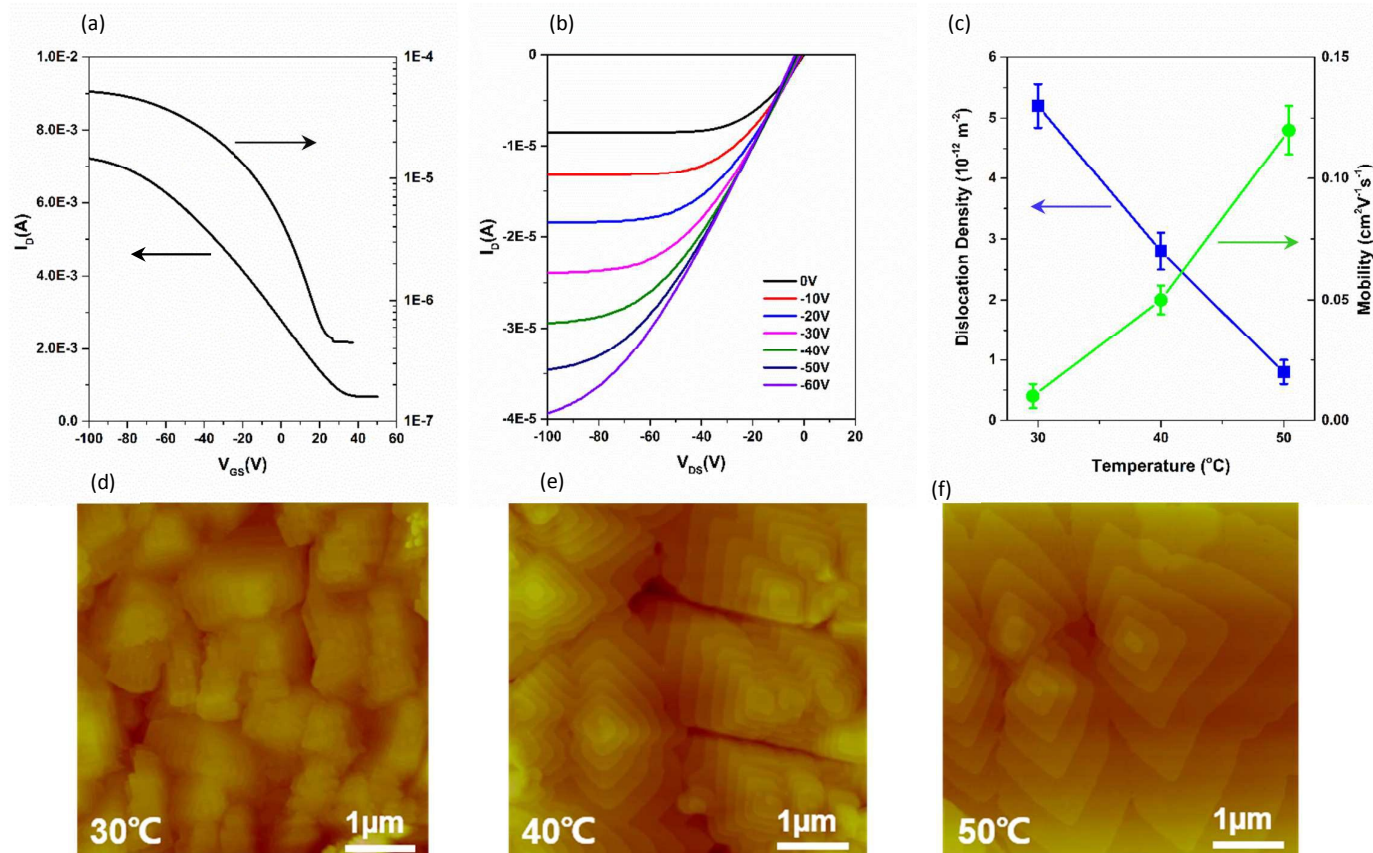


Figure 5. Device performance of DMDPC thin film. (a)  $I_{DS}$ - $V_{GS}$  characteristics at  $V_{DS}=-100\text{V}$ . (b)  $I_{DS}$ - $V_{DS}$  characteristics of the device in (a). From top to bottom,  $V_G=0\text{V}$ ,  $-10\text{V}$ ,  $-20\text{V}$ ,  $-30\text{V}$ ,  $-40\text{V}$ ,  $-50\text{V}$  and  $-60\text{V}$ , respectively. (c) The fitting curves of dislocation density and mobility changing with substrate temperature. (d-f)  $5\mu\text{m} \times 5\mu\text{m}$  AFM images of DMDPC films with nominal 45 nm deposited with three different substrate temperature.

As to the fabrication of TFTs, 45nm DMDPC films were deposited onto the OTS treated substrate at room temperature. Source and drain electrodes were formed by evaporating 50nm gold films through a shadow mask with channel length  $L=50\mu\text{m}$  and width  $W=1000\mu\text{m}$ . Electrical characterization of devices was measured in air by a Keithley 4200 semiconductor analyzer. The fabricated devices were measured in atmosphere at room temperature. Shown in Figure 5a are the typical transfer current-voltage curves, from which a field-effect mobility of  $0.08\text{cm}^2\text{V}^{-1}\text{s}^{-1}$  was measured in the saturation regime using the equation:  $I_{SD} = (\mu WC_i/2L)(V_G - V_T)^2$ , where  $I_{SD}$  is the drain current,  $\mu$  is mobility,  $C_i$  is the capacitance per unit area for OTS-treated  $\text{SiO}_2$  substrate,  $W$  is the channel width,  $L$  is the channel length,  $V_G$  and  $V_T$  are the gate and threshold voltage, respectively. In addition, the device presented the high off-current and the relative low on/off ratio. One possible explanation is that the channel between the semiconductor and the substrate was doped by the air (see supporting information S2). Shown in Figure 5b are the typical output curves for the DMDPC TFTs. Compared to the un-optimized condition that the deposition rate was

$1\text{nm}/\text{min}$  and the substrate was bare  $\text{SiO}_2$ , the device performance was at poor level with mobility of  $1.3 \times 10^{-3} \text{cm}^2 \text{V}^{-1} \text{s}^{-1}$  (see supporting information S3).

The grain size and grain boundary have great influence on the performance of thin film transistors.<sup>28</sup> In this context, we systematically examined the grain size of DMDPC spirals under different substrate temperature. As shown in Figure 5d, 5e, 5f, three different substrate temperature  $30^{\circ}\text{C}$ ,  $40^{\circ}\text{C}$  and  $50^{\circ}\text{C}$  exhibited different grain size. The higher substrate temperature results in larger grain size. The mobility of the fabricated DMDPC-based OTFTs were found to be related to the SSD grain size. The grain size can be extracted from the initial nucleation densities which can be fitted through the Equation (1):<sup>29</sup>

$$N = R^p \exp\left(\frac{-E_{des} + E_{diff} + \Delta G}{kT_s}\right), \quad (1)$$

Where  $N$  is the nucleation density,  $R$  is the deposition rate,  $p$  is a parameter related with the critical nucleus size which can be simulated as a constant in our experiments.  $k_B$  is Boltzmann constant,  $T_s$  is the substrate temperature,  $E_{des}$  is the energetic

barrier to desorption,  $E_{\text{diff}}$  is the energetic barrier to diffusion, and the  $\Delta G$  is the thermodynamic barrier required to form a stable island.

As the substrate temperature was increasing, the chance was higher for molecules to encounter another to form a stable cluster and the deposited molecules had a longer migration distance to form bigger DMDPC domains, leading to the increasing grain size and lower nucleation density. Figure 5c shows the dependence between dislocation density and substrate temperature, the dislocation density decreases with the increasing substrate temperature  $T_s$ , which indicates that using substrate temperature to control the grain size of DMDPC thin films is effective. We also systematically discussed the influence of deposition rate on the FET performance (supporting information S4, S5). The lower dislocation density means the lower nucleus density and larger grain size. The mobility of the fabricated thin film transistors for the increasing substrate temperature are 0.01, 0.05 and 0.12  $\text{cm}^2\text{V}^{-1}\text{s}^{-1}$ , respectively. With the substrate temperature increasing, the grain size could increase and the relevant grain boundary decrease which contributed to the higher mobility.

## Conclusions

In conclusion, spirals of organic thin films were synthesized using a directly physical vapor deposition (PVD) method. The DMDPC films were optimized to follow a screw dislocation driven growth mode. By the aid of the OTS treated substrate and low deposition rate as well as elevated substrate temperature, key screw dislocation features including monolayer steps and helical fringes were observed to support the spiral growth. Schematic models were drawn to illustrate how the screw dislocations generate and propagate. Moreover, fabricated thin film transistors possess the device performance with hole mobility up to 0.12  $\text{cm}^2\text{V}^{-1}\text{s}^{-1}$ . The dependent of mobility with grain size of spirals were discussed. This work shed light on the understanding of spiral growth mechanism of organic thin films, which might be helpful to optimize the organic electronic devices.

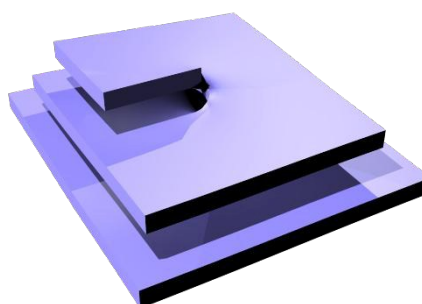
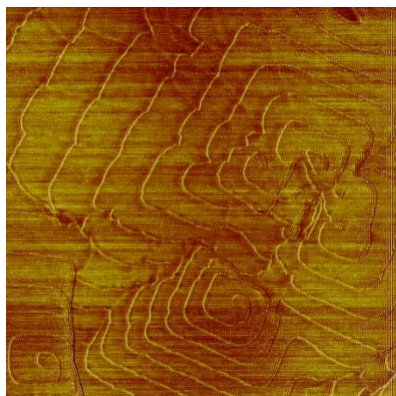
## Acknowledgements

This study was supported by the grant from the National Natural Science Foundation of China (Grant Nos. 11374070, 61327009, and 21432005), and the "Strategic Priority Research Program" of the Chinese Academy of Sciences (Grant No. XDA 09040201).

## References

1. R. A. Street, *Adv Mater*, 2009, **21**, 2007-2022.
2. T. Someya, T. Sekitani, S. Iba, Y. Kato, H. Kawaguchi and T. Sakurai, *P Natl Acad Sci USA*, 2004, **101**, 9966-9970.
3. T. D. Anthopoulos, S. Setayesh, E. Smits, M. Colle, E. Cantatore, B. de Boer, P. W. M. Blom and D. M. de Leeuw, *Adv Mater*, 2006, **18**, 1900-+.
4. J. Zaumseil and H. Sirringhaus, *Chem Rev*, 2007, **107**,

5. 1296-1323.
6. A. A. Virkar, S. Mannsfeld, Z. A. Bao and N. Stingelin, *Adv Mater*, 2010, **22**, 3857-3875.
7. G. Horowitz, *Adv Funct Mater*, 2003, **13**, 53-60.
8. Y. Y. Hu, L. M. Wang, Q. Qi, D. X. Li and C. Jiang, *J Phys Chem C*, 2011, **115**, 23568-23573.
9. S. Verlaak, S. Steudel, P. Heremans, D. Janssen and M. S. Deleuze, *Phys Rev B*, 2003, **68**.
10. D. W. He, Y. A. Zhang, Q. S. Wu, R. Xu, H. Y. Nan, J. F. Liu, J. J. Yao, Z. L. Wang, S. J. Yuan, Y. Li, Y. Shi, J. L. Wang, Z. H. Ni, L. He, F. Miao, F. Q. Song, H. X. Xu, K. Watanabe, T. Taniguchi, J. B. Xu and X. R. Wang, *Nat Commun*, 2014, **5**.
11. R. Ruiz, D. Choudhary, B. Nickel, T. Toccoli, K. C. Chang, A. C. Mayer, P. Clancy, J. M. Blakely, R. L. Headrick, S. Iannotta and G. G. Malliaras, *Chem Mater*, 2004, **16**, 4497-4508.
12. M. Mas-Torrent and C. Rovira, *Chem Soc Rev*, 2008, **37**, 827-838.
13. Z. X. Liang, Q. Tang, R. X. Mao, D. Q. Liu, J. B. Xu and Q. Miao, *Adv Mater*, 2011, **23**, 5514-+.
14. H. Klauk, *Chem Soc Rev*, 2010, **39**, 2643-2666.
15. L. M. Zhang, K. H. Liu, A. B. Wong, J. Kim, X. P. Hong, C. Liu, T. Cao, S. G. Louie, F. Wang and P. D. Yang, *Nano Lett*, 2014, **14**, 6418-6423.
16. L. Chen, B. L. Liu, A. N. Abbas, Y. Q. Ma, X. Fang, Y. H. Liu and C. W. Zhou, *Acs Nano*, 2014, **8**, 11543-11551.
17. S. A. Morin and S. Jin, *Nano Lett*, 2010, **10**, 3459-3463.
18. S. A. Morin, M. J. Bierman, J. Tong and S. Jin, *Science*, 2010, **328**, 476-480.
19. J. Wang, D. K. Qin, J. B. Lan, Y. Y. Cheng, S. Zhang, Q. Guo, J. Wu, D. Wu and J. S. You, *Chem Commun*, 2015, **51**, 6337-6339.
20. M. L. Tang, T. Okamoto and Z. N. Bao, *J Am Chem Soc*, 2006, **128**, 16002-16003.
21. B. Nickel, R. Barabash, R. Ruiz, N. Koch, A. Kahn, L. C. Feldman, R. F. Haglund and G. Scoles, *Phys Rev B*, 2004, **70**.
22. W. K. Burton, N. Cabrera and F. C. Frank, *Philos TR Soc S-A*, 1951, **243**, 299-358.
23. Z. B. Kuvadia and M. F. Doherty, *Cryst Growth Des*, 2011, **11**, 2780-2802.
24. R. C. Snyder and M. F. Doherty, *P R Soc A*, 2009, **465**, 1145-1171.
25. J. D. Rimer, Z. H. An, Z. N. Zhu, M. H. Lee, D. S. Goldfarb, J. A. Wesson and M. D. Ward, *Science*, 2010, **330**, 337-341.
26. P. Dandekar, Z. B. Kuvadia and M. F. Doherty, *Annu Rev Mater Res*, 2013, **43**, 359-386.
27. J. Fujita, S. Kuroshima, T. Satoh, J. S. Tsai, T. W. Ebbesen and K. Tanigaki, *Appl Phys Lett*, 1993, **63**, 1008-1010.
28. M. Beigmohamadi, P. Niyamakom, A. Farahzadi, S. Kremers, T. Michely and M. Wuttig, *Phys Status Solidi-R*, 2008, **2**, 1-3.
29. Y. W. Zhang, D. X. Li and C. Jiang, *Appl Phys Lett*, 2013, **103**.
30. J. A. Venables, G. D. T. Spiller and M. Hanbucken, *Rep Prog Phys*, 1984, **47**, 399-459.

**Abstract**

We report the observation of a screw-dislocation-driven spiral growth of DMDPC organic thin films using a physical vapor deposition. The existence of screw dislocations was clearly confirmed by the observations of outcropped steps, single monolayer height helical periodicity and spiral fringes. AFM force image showing obvious helical fringes and spirals.